Low-Power, Phase-Preserving 2R Amplitude Regenerator

Taras I. Lakoba* and Jake R. Williams

Dept. of Mathematics and Statistics, University of Vermont, Burlington, VT 05401

Michael Vasilyev

Dept. of Electrical Engineering, University of Texas at Arlington, Arlington, TX 76019

Abstract

We propose a modification of a NALM-based 2R regenerator of phase-encoded signals which operates at considerably lower input powers than was studied earlier. Our modification consists of replacing the core-matched and lossless fiber coupler in the NALM by a coupler with a propagation constant mismatch and loss asymmetrically distributed between the two cores. The performance of the modified regenerator and the one studied earlier is approximately the same.

Keywords: phase-preserving 2R regeneration; nonlinear amplifying loop mirror; mismatched fiber coupler.

1   Introduction

All-optical 2R regeneration (re-amplification and re-shaping) is an important technology for the development of next-generation optical networks, and many different 2R architectures have been proposed and demonstrated [1], including ones based on nonlinear interferometers, on self-phase- or cross-phase-modulation (SPM or XPM, respectively) followed by spectral filtering, on gain saturation or saturable absorption, etc. While the 2R regenerator based on SPM followed by spectral filtering [2]–[4] is the simplest and most robust choice for processing on-off keying signals, it is not suitable for phase-encoded data, because of its propensity to dramatically increase the phase fluctuations through intensity-to-phase noise conversion. On the other hand, the regenerators based on nonlinear fiber interferometers [5, 6], after some modification, have a potential for processing phase-encoded signals.

Recently, a 2R regeneration scheme for phase-encoded signals based on a nonlinear amplifying loop mirror (NALM) was proposed and investigated [7]–[11]. Such a regenerator is capable of suppressing amplitude jitter without affecting the phase of the signal. This improves the signal quality in two ways. First, since both amplitude and phase fluctuations affect the

---

*Corresponding author: tlakoba@uvm.edu, 1 (802) 656-2610

eye opening of a phase-encoded signal at the receiver, suppression of the amplitude jitter increases the eye opening and hence reduces the bit error rate (BER). Second, the fiber's Kerr nonlinearity converts amplitude fluctuations into phase ones, which then rapidly accumulate with the propagation distance [12]. Such phase fluctuations caused by the Gordon-Mollenauer effect are often referred to as nonlinear phase noise. Then, reducing the fluctuations at, say, the midpoint of the transmission line will prevent creation and accumulation of the nonlinear phase noise. This will further reduce the BER of the received signal. Effectiveness of the NALM for regenerating phase-encoded signals was demonstrated numerically [7, 8] and experimentally [9, 10, 13].

A drawback of the NALM-based regenerator described above is a high input (and output) power required for its operation. For example, for the parameters similar to those used in [13], the input peak power is about 200 mW, and output peak power is higher than 10 W; see Fig. 2 below. However, only on the order of 1 to 10 mW of the regenerator's output can be relaunched into the transmission line; the rest of the output will have to be damped (i.e. wasted). A method to shift the operation point of the NALM in order to lower those high powers was proposed in [11]. It is based on adjusting the signal polarization inside the NALM (a similar principle was earlier proposed in [14, 15] for a different application). However, if the NALM-based regenerator is to be used in telecom applications, active adjustment of polarization in it would be impractical.

In this paper we propose a different method of shifting the NALM's operating point, which does not require control of either polarization or any other quantity that would be difficult to monitor in a telecom application. Our method, instead, requires a modification of the fiber coupler in the NALM. Specifically, we propose to use a coupler whose two cores have different propagation constants and, in addition, one (but not both!) of the cores has a considerable amount of dissipation. Most commercial applications require that precisely these properties of the coupler — the core mismatch and dissipation — be minimized, i.e. the cores are to be identical and should exhibit no losses [16]. It is, therefore, surprising that these usually undesirable properties of the coupler allow one to reduce the input power to a NALM-based regenerator by almost two orders of magnitude.

In what follows we will use a shorthand for a coupler without the loss and dissipation, referring to it as the "conventional" coupler, as opposed to the modified coupler whose utilization we propose in this work.

In Section 2 we outline a theory of a NALM with the modified coupler and estimate what parameters of the coupler would allow one to shift the regeneration point into the low-power regime. In Section 3 we verify these estimates by numerical simulations that account for both the nonlinearity and the dispersion of the NALM's highly nonlinear fiber (HNLF). In particular, we determine ranges of the coupler's parameters where phase-preserving amplitude regeneration with low input power is achievable. We also show that the eye opening of the signals regenerated in this low-power regime and in the high-power regime considered in [7], [9]–[11], [13] is about the same.

2 Theory of a NALM-based regenerator with the modified coupler

In this section we will: (i) Present a transfer matrix of a coupler with mismatched cores and asymmetric dissipation; (ii) Derive equations of a NALM with such a coupler; (iii) Estimate the range of the coupler's parameters where the NALM can act as a regenerator for low input power, and (iv) Verify these estimates by a quick simulation that ignores fiber dispersion.

2.1 Modified coupler

The standard coupled-mode equations of a coupler in question are (see, e.g., [17], [18]):

$$\partial_z \mathcal{E}_1 = i\Delta \mathcal{E}_1 + i\kappa \mathcal{E}_2$$
$$\partial_z \mathcal{E}_2 = i\kappa \mathcal{E}_1 - (i\Delta + \mu)\mathcal{E}_2 \ . \tag{1}$$

Here $\mathcal{E}_{1,2}$ are the electric fields in the two cores of the coupler, κ and Δ are the coupling and propagation-constant mismatch between the cores, and μ is the dissipation introduced into one of the cores. The solution to these equations is:

$$\begin{pmatrix} \mathcal{E}_1 \\ \mathcal{E}_2 \end{pmatrix}_{\text{out}} = e^{-\mu z/2} \begin{pmatrix} \cos\rho z + i\sin\psi \, \sin\rho z & i\cos\psi \sin\rho z \\ i\cos\psi \, \sin\rho z & \cos\rho z - i\sin\psi \, \sin\rho z \end{pmatrix} \begin{pmatrix} \mathcal{E}_1 \\ \mathcal{E}_2 \end{pmatrix}_{\text{in}}, \tag{2a}$$

where

$$\rho = \kappa\sqrt{1+(x+iy)^2}, \quad x = \frac{\Delta}{\kappa}, \quad y = \frac{\mu}{2\kappa}, \quad \sin\psi \equiv \frac{\Delta + i\mu/2}{\rho}, \quad \cos\psi \equiv \frac{\kappa}{\rho}. \tag{2b}$$

Thus, ρ and ψ are, in general, complex-valued parameters. Note that while dissipation acts only in one of the cores, it reduces the energies of the field in both cores via coupling. In the absence of core mismatch, one has $x = y = 0$ and hence $\rho = \kappa$ and $\psi = 0$. Then $\cos^2 \kappa z : \sin^2 \kappa z$ is the power-splitting coefficient of the conventional coupler.

Let us now comment on the feasibility of experimental implementation of a coupler governed by Eqs. (1). Core mismatch can be achieved by using cores with slightly different diameters. Dissipation can be introduced into one of the cores by, e.g., writing a long-period Bragg grating which can be designed to excite a leaky mode cause energy loss. Since this modification of the coupler can be implemented without breaking the circular symmetry of the cores' cross-sections, then it will not introduce polarization dependence to the coupler. Thus, at least conceptually, such a modified coupler will not require any polarization control inside the NALM, as we have announced in the introduction.

2.2 Equations of the NALM and their analysis

The fields immediately after the coupler (see Fig. 1) satisfy:

$$\begin{pmatrix} E_3 \\ E_4 \end{pmatrix}_{\text{in}} = A \begin{pmatrix} E_1 \\ E_2 \end{pmatrix}_{\text{in}} \equiv A \begin{pmatrix} E \\ 0 \end{pmatrix}, \tag{3}$$

where A is the product of $\exp(-\mu z/2)$ and the matrix in (2a). Upon passing through the loop and just before the coupler, these fields become

$$(E_{3,4})_{\text{out}} = \sqrt{G}(E_{3,4})_{\text{in}} \exp(i\phi_{3,4}), \tag{4}$$

provided that the HNLF's dispersion has been ignored. The phases $\phi_{3,4}$, acquired due to the fields' passing through the HNLF, are:

$$\phi_3 = \gamma L \left(|E_{3\text{in}}|^2 + 2G\overline{|E_{4\text{in}}|^2} \right)$$
$$\phi_4 = \gamma L \left(G|E_{4\text{in}}|^2 + 2\overline{|E_{3\text{in}}|^2} \right). \tag{5}$$

Here γ and L are the nonlinearity coefficient and length of the HNLF and G is the gain of the amplifier inside the loop. In the first of Eqs. (5), the first term occurs due to SPM of the signal, and the second term, due to XPM by the counter-propagating signal, and similarly for the second equation. The overbar denotes time averaging: thus, $|E|^2$ denotes instantaneous power, while $\overline{|E|^2}$ stands for its time-averaged value. If, furthermore, we identify $|E|^2$ with the signal's peak power, then for phase-encoded signals,

$$\overline{|E|^2} = d\,|E|^2, \tag{6}$$
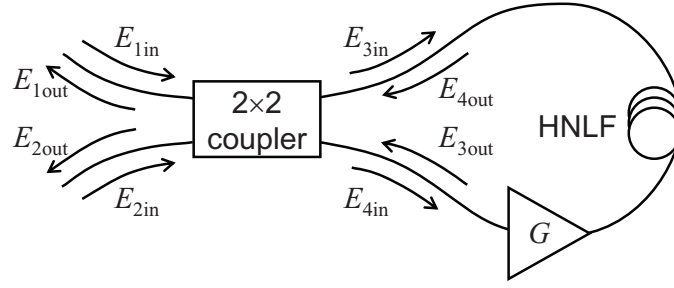
where d is the duty cycle of the pulses.

Figure 1: Schematics of the NALM-based regenerator.

The fields at the output of the NALM are found from a counterpart of (3):

$$\begin{pmatrix} E_1 \\ E_2 \end{pmatrix}_{\text{out}} = A \begin{pmatrix} E_4 \\ E_3 \end{pmatrix}_{\text{out}}. \tag{7}$$

Note that in writing (7), the asymmetry of the coupler due to dissipation being present only in one of its cores (see (1)) dictates the order in which the fields enter the equation. That is:

$$\begin{pmatrix} E_2 \\ E_1 \end{pmatrix}_{\text{out}} \neq A \begin{pmatrix} E_3 \\ E_4 \end{pmatrix}_{\text{out}}. \tag{8}$$

Using Eqs. (2)–(7), one obtains the following expressions for the output fields:

$$E_{2\text{out}} = e^{-\mu z}\sqrt{G} \left[(\cos^2 \rho z + \sin^2 \psi \sin^2 \rho z)e^{i\phi_3} - (\cos^2 \psi \sin^2 \rho z)e^{i\phi_4} \right] E, \tag{9a}$$

$$E_{1\text{out}} = e^{-\mu z} i\sqrt{G} \cos \psi \sin \rho z \, (\cos \rho z + i \sin \psi \sin \rho z)(e^{i\phi_3} + e^{i\phi_4})E. \tag{9b}$$

Field $E_{1\text{out}}$ is that reflected by the NALM, while $E_{2\text{out}}$ is the one transmitted. It is interesting to note that for $\mu \neq 0$, $|E_{1\text{out}}|^2 + |E_{2\text{out}}|^2 \neq G|E|^2 \exp{(-2\mu z)}$, and moreover, even $|E_{3\text{in}}|^2 + |E_{4\text{in}}|^2 \neq |E|^2 \exp{(-\mu z)}$.

4

Before analyzing how the regenerated signal $E_{2\text{out}}$ depends on parameters Δ and μ in (1), we state its form for the conventional coupler, i.e. that with $\Delta = \mu = 0$ (and hence with $\rho = \kappa$), used in earlier studies:

$$E_{2\text{out}} = \sqrt{G} \left(\cos^2 \kappa z \, e^{i\phi_3} - \sin^2 \kappa z \, e^{i\phi_4} \right) E.$$ (10)

In Fig. 2 we show (with the solid line) the corresponding peak power, $|E_{2\text{out}}|^2$, and phase,

$$\arg\left(E_{2\text{out}}\right) - 2\gamma L \left(\overline{|E_{3\text{in}}|^2} + G\overline{|E_{4\text{in}}|^2} \right);$$ (11)

in Appendix A we explain the reason for subtracting the last term in (11). Parameters for the plots in Fig. 2 are similar to those used in, e.g., [13]: $\gamma = 2.5 \text{ W}^{-1}\text{km}^{-1}$, $L = 2$ km, $d = 0.05$ (5-ps pulses with 10 Gb/s repetition rate), $G = 100$, and $\kappa z = 0.33$ (corresponding to the power-splitting ratio of the coupler of $\cos^2 \kappa z : \sin^2 \kappa z \approx 0.90 : 0.10$). The range of input powers — $|E_{1\text{in}}|^2$ from about 0.12 to about 0.14 W in this case — where the power and phase plateaus overlap, is the operating range of the NALM-based regenerator. This is because both the power and phase of regenerated pulses remain almost constant for any value of the input power $|E_{1\text{in}}|^2$ within such a range. The interval of κz values where these plateaus overlap is, for the parameters listed above, approximately (0.30, 0.40).
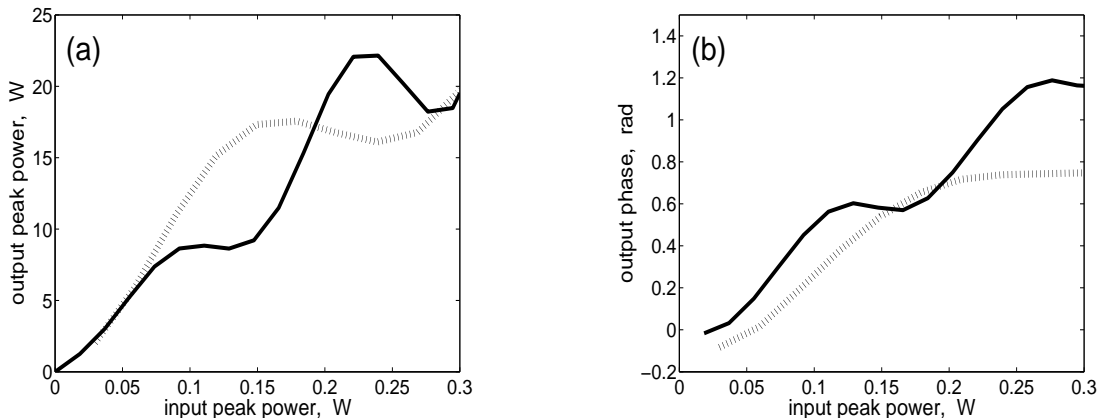

Figure 2: Power (a) and phase (b) transfer curves of the earlier studied model with a "conventional" coupler with no core mismatch and no dissipation ($\Delta = 0$, $\mu = 0$). The solid and dotted lines correspond to the dispersionless and dispersive cases considered in Secs. 2 and 3, respectively. Parameter κz equals 0.33 and 0.38 in the dispersionless and dispersive cases, respectively, and the other parameters are specified in the text.

Below we discuss how parameters μ and Δ in (1) should be chosen to shift the operating power of the regenerator to a significantly lower value. We will first show how to shift the plateau in the power transfer curve, and then indicate how the plateau in the phase curve can be shifted along. For low input powers, when ϕ_3 and ϕ_4 are close to zero, so is the relative phase between the two terms in (10):

$$\arg\left(e^{i\phi_3} \cos^2 \kappa z\right) - \arg\left(e^{i\phi_4} \sin^2 \kappa z\right) \approx 0.$$ (12a)

As Fig. 2 illustrates, there is no plateau in the power transfer curve for low input powers. Instead, the plateau occurs when the phase difference between the aforementioned terms approaches π:

$$\arg\left(e^{i\phi_3}\cos^2\kappa z\right) - \arg\left(e^{i\phi_4}\sin^2\kappa z\right) \approx \pi. \tag{12b}$$

This observation provides a hint as to how μ and Δ need to be chosen in (1) to create a power plateau at low input powers. Namely, the relative phase between the two terms in (9a) needs to be close to π:

$$\arg\left(\cos^2\rho z + \sin^2\psi\sin^2\rho z\right) - \arg\left(\cos^2\psi\sin^2\rho z\right) \approx \pi, \tag{13}$$

where we have used the fact that for low input powers, $\exp\left(i\phi_3\right) \approx \exp\left(i\phi_4\right) \approx 1$. Having chosen μ and Δ so as to ensure the key relation (13), we will then verify, by inspection, whether the phase transfer curve has a plateau in a range of input powers where the power transfer curve does.

As a first step in implementation of the program outlined above, we note that if $\mu = 0$ and $\Delta \neq 0$, then in (2b), ρ and ψ are real, and hence (13) cannot be satisfied. Next, since the case where both μ and Δ are nonzero is too complicated, we now analytically consider the case $\mu \neq 0$, $\Delta = 0$ and will later explore numerically the consequences of having $\Delta \neq 0$. For $\mu \neq 0$ and $\Delta = 0$, $\sin\psi$ is purely imaginary, while $\cos\psi$ is real (provided that $y = \mu/2\kappa < 1$, which we will always assume in order not to have too much dissipation in the coupler). Then (13) will be satisfied when

$$\cos^2\rho z - |\sin^2\psi|\sin^2\rho z \ < \ 0, \tag{14}$$

which requires that: (i) ρz be close to $\pi/2$ and (ii) $|\psi|$ be not too small. Making these general, but rather vague, recommendations precise requires numerical simulations, which should also include the effect of $\Delta \neq 0$ on the power and phase transfer curves.

In Fig. 3 we plot such curves, obtained from Eqs. (9), for selected values of parameters x, y, κz (see (2b)). As announced earlier, the input powers required for plateau existence are on the order of a few milliwatts, i.e. more than an order of magnitude less than required for the earlier-studied setup; compare with Fig. 2. As a side note, let us point out that flatter plateaus can be obtained if one adjusts the value of x for a given value of y. However, in Fig. 3 we intended to emphasize that a single value of x can work for a *range* of y values.

Another potentially useful property of the regenerator with the modified coupler is that it is much less demanding of the gain G of the amplifier inside the NALM (see Fig. 1). In [11] it was pointed out that the regenerator with the conventional coupler must employ an amplifier with gain of at least 17 dB to achieve simultaenous plateaus in the power and phase transfer curves. We actually observed eye opening improvement (see Sec. 3) of about 1.0 dB of a signal regenerated by the earlier-studied setup with $G = 13$ dB, but were unable to obtain any considerable eye opening when the gain became less than 10 dB. On the other hand, the regenerator with the modified coupler can operate even with G as low as 3 dB. The corresponding transfer curves look similar to those shown in Fig. 3 and therefore are not displayed; the only obvious difference is that the input power is greater than in Fig. 3 by a factor between 50 and 100.
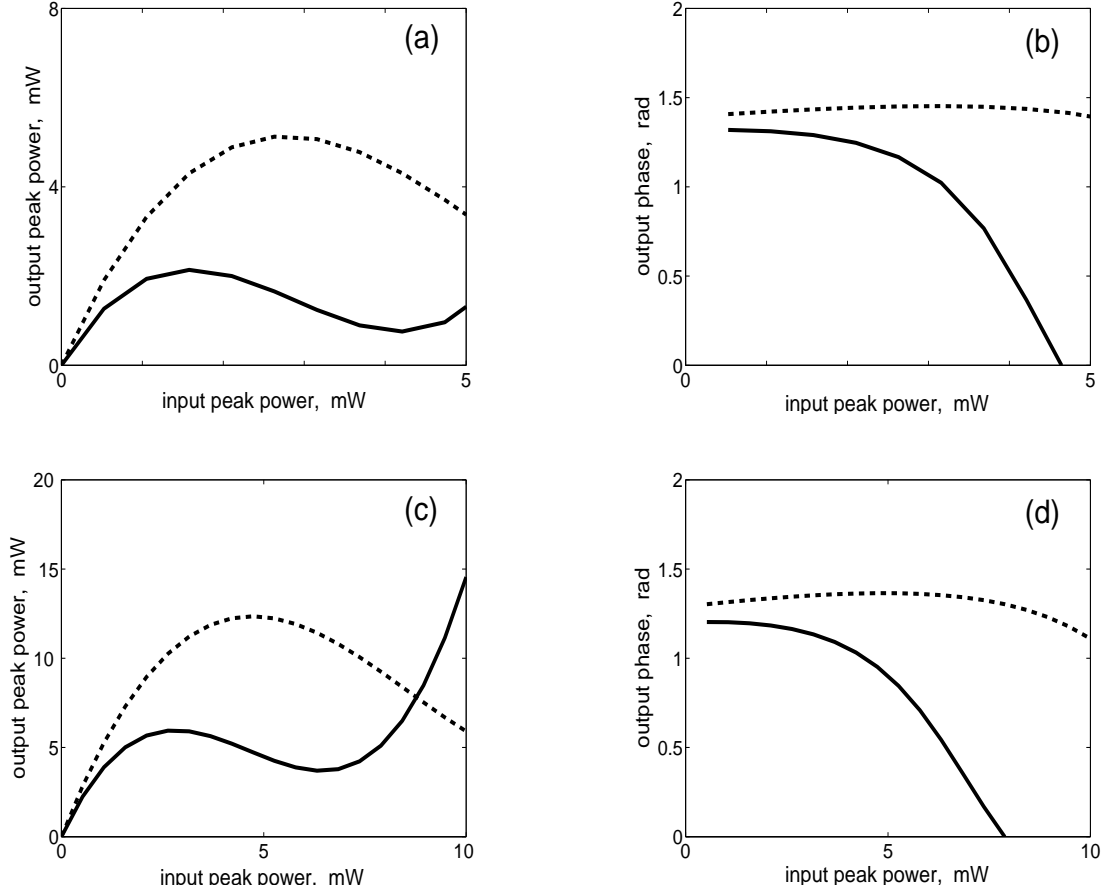
Figure 3: Power (a), (c) and phase (b), (d) transfer curves of a dispersionless regenerator employing the modified coupler with: $\kappa z = 1.3$, $x = 1.0$ (a), (b); $\kappa z = 1.6$, $x = 0.85$ (c), (d). The solid and dashed curves correspond to $y = 0.2$ and $y = 0.3$, respectively. Note that the horizontal scale here is in milliwatts, while in Fig. 2 it is in watts.

We now comment on the amount of energy loss occurring in the coupler. The signal power after passing through the coupler once is proportional to $\exp(-\mu z)$. Thus, for $\kappa z = 1.3$ and $y = 0.3$, $\mu z = 2\kappa z \cdot y \approx 0.78$, so that energy dissipation after one pass through the coupler is less than 3.5 dB. Even smaller dissipation — less than 2.5 dB — would occur for $\kappa z = 1.3$ and $y = 0.2$. This rather moderate amount of energy loss may be a reasonable alternative to using a much higher input power.

To conclude this section, let us emphasize that the regenerator's operating in a low power regime by no means suggests that this regime is linear. It is evident from Fig. 3 that a certain minimum power is still required for the existence of the plateau in the power transfer curves. This minimum power is considerably lower than that in the regenerator proposed in [7] because for the regenerator with the modified coupler, the "birth" of the plateau is facilitated by relation (13).

3 Numerical verification

Here we will first consider the effect of dispersion of the NALM's HNLF on the solutions obtained in the previous section. Then we will demonstrate that the NALM-based regenerator with a coupler described by (1) can indeed improve the quality of differential phase-shift-keyed signals. As in Sec. 2, we use the regenerator parameters as in [13], explicitly listed after our Eq. (11). In addition to these parameters, we set the fiber dispersion to -2 ps/nm/km and postcompensate the output signal by 4 ps/nm. To account for the fiber dispersion, we solve the nonlinear Schrödinger equation with input fields $(E_{3,4})_{\text{in}}$ instead of using Eqs. (4), (5).

The respective counterparts of results for the dispersionless cases depicted in Figs. 2 (solid lines) and 3 are shown in Figs. 2 (dotted lines) and 4. For the earlier-studied regenerator employing a coupler with no mismatch and dissipation, fiber dispersion is seen to have a considerable effect on the transfer curves; note also that the coupler splitting-ratio parameter κz had to be adjusted to reduce the differences between the curves in the dispersionless and dispersive regimes. On the contrary, dispersion is seen to have only minor effect on the transfer curves for the regenerator employing a modified coupler.
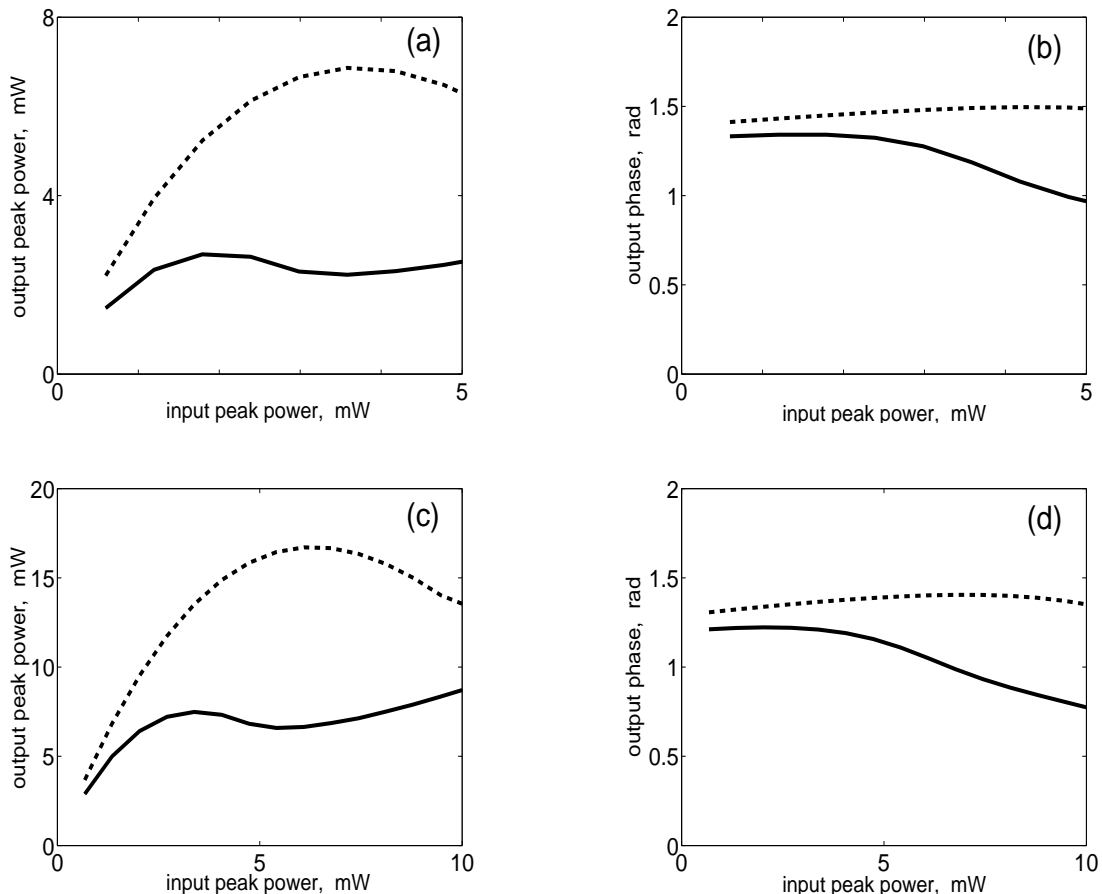

Figure 4: Same as in Fig. 3, but for a NALM with fiber dispersion of -2 ps/nm/km.

In Fig. 5 we show the input and regenerator signals to the regenerators employing the conventional and modified couplers. The simulated input is a $2^7 - 1$-pulse pseudo-random bit

sequence with amplitude jitter of $\pm 30\%$ and no phase jitter. The is no optical filter at the receiver, and the electrical filter's bandwidth is 20 GHz. The values of the coupler parameters and the average[1] input peak powers are listed in the caption to Fig. 5, and the remaining parameters have been listed earlier in Secs. 2 and 3. The eye opening is measured with respect to a 3-ps "window" fitted inside the electrical eye, with the input and regenerated signals being normalized to have the same time-averaged power. The eye openings of the outputs of the regenerators with the conventional (Fig. 5b) and modified (Fig. 5c) coupler are both 1.0 dB. The former "eye" looks a little noisier, but results in the same eye opening improvement as the latter "eye", because the regenerated pulses in the former case are slightly narrower than those in the latter case.
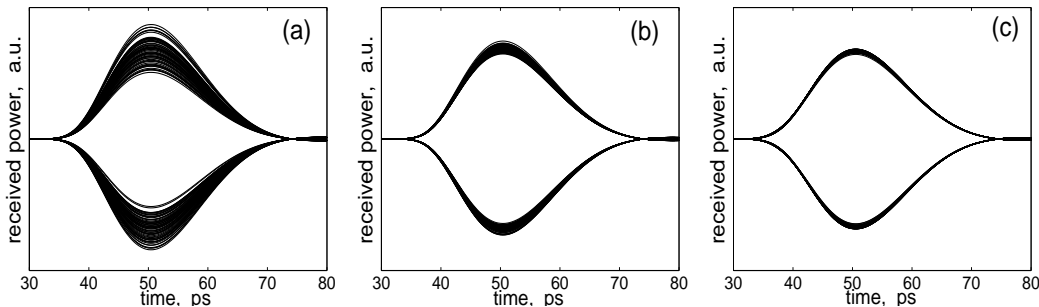

Figure 5: Electrical eye diagrams of the input (a) and regenerated (b), (c) signals. For (b): $x = y = 0$ (the conventional coupler), $\kappa z = 0.38$, average (over all pulses) peak $|E|^2 = 220$ mW; for (c): $x = 1.0$, $y = 0.2$, $\kappa z = 1.3$, average peak $|E|^2 = 2.6$ mW.

Following up on the observation, made in Sec. 2, that the regenerator with a modified coupler can operate with the amplifier's gain in the NALM being as low as 3 dB, we also simulated the case with the same parameters as in Fig. 5c except that $G = 3$ dB. For the input peak powers in the range from 190 to 230 mW, we found the eye opening of the regenerated signal to be at least 1.0 dB. (The eye diagram looks almost identical to that in Fig. 5c.) The above range of input power is comparable to that for the regenerator with the conventional coupler, but now the device uses a low-gain amplifier and hence still has considerably lower energy consumption than that studied in [7]–[11], [13].

Finally, in Fig. 6 we illustrate how varying the modified coupler's parameters affects the performance of the regenerator. For a given pair $(y, \kappa z)$, we searched for such a value of the input power that the interval of x-values where the eye opening is at least 1.0 dB, is the widest. The endpoints of those intervals are plotted in Fig. 6a and the corresponding input peak powers, in Fig. 6b. If the input power deviates slightly from the plotted optimal value, than $x_{\min}$ and $x_{\max}$ also change, but the width, $x_{\max} - x_{\min}$, of the x-interval, remains approximately the same. If we now remove the restriction that the input power be fixed for all the x values in those intervals, but instead adjust it for each given x, then, naturally, the range of the corresponding x values for a given pair $(y, \kappa z)$ is wider than shown in Fig. 6a.

---

[1]Note the difference between two similar terms. *Average peak power* refers to the averaging over peak powers of all pulses; it does not depend on the duty cycle d. In contrast, *time-averaged power* refers to the averaging of the signal power over time and is proportional to d.
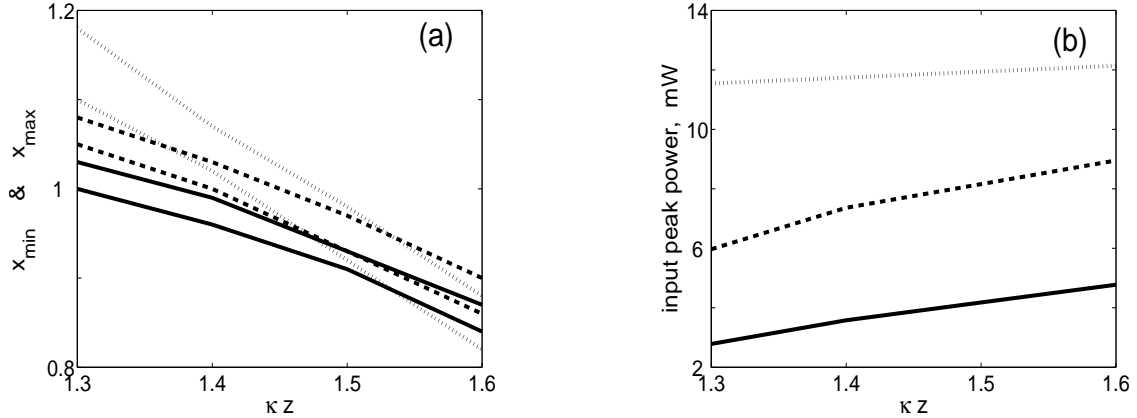
Figure 6: (a) Minimum and maximum x-values of the modified coupler for which the regenerator produces eye opening of at least 1.0 dB; (b) the corresponding input powers. Solid, dashed, and dotted lines correspond to $y = 0.2$, 0.3, and 0.4, respectively.

4 Conclusions

We have proposed a method to reduce by more than an order of magnitude the input power to the phase-preserving 2R amplitude regenerator studied in [7]–[11], [13]. Our method is based on replacing the conventional fiber coupler in the NALM of that regenerator by a coupler with certain amounts of propagation constant mismatch between, and asymmetric dissipation in, the two cores, as described by Eqs. (1). Such a modification to the coupler does not require any polarization control. The reason why the input power required for regeneration is considerably lower than in the previously studied setup is explained around Eq. (13). Namely, the additional degrees of freedom provided by the modified coupler enable — already at low operating powers — approximately a π-shift between the phases of the fields interfering at the NALM's output, whereas with the conventional coupler, such a shift can only be attained at high power.

We have demonstrated that the performance of the regenerators with the modified and conventional couplers is approximately the same; see Fig. 5 and the text about it. Moreover, the operation of the regenerator with the modified coupler does *not*, unlike that of the device with the conventional coupler, require a high-gain amplifier inside the NALM. In fact, the former regenerator can operate with the amplifier's gain being as low as 3 dB, whereas the latter one requires at least 17 dB [11, 13]. Let us stress that even more important than a lower gain is the lower output power of the amplifier, since it is this parameter that drives the amplifier's cost. As we demonstrated in Sec. 3, the output power in the NALM with the modified coupler (which cannot exceed the product of the input power and gain G) is one to two orders of magnitude lower than that in the NALM with the conventional coupler, regardless of the exact value of the amplifier's gain inside the loop. Thus, employing the modified coupler has the potential to make the device proposed in [7] more cost-effective and hence more practical.

Acknowledgement

Appendix A: Justification of the subtracted term in (11)

We will present this justification at two levels. First, we will explain the motivation for subtracting a certain term from $\arg(E_{2\text{out}})$. Then, we will explain why that term should be exactly as indicated in (11).

The term in question corresponds to the phase contributions from the XPM by the counter-propagating signals (see the text after (5)). This contribution is determined by the time-averaged signal power and therefore does not affect the *relative* phase of any two *adjacent* regenerated pulses. Hence its inclusion (or not) in the definition of phase does not affect the eye opening of a signal with a given average input power, which is the measure of the regenerator performance presented in Sec. 3. On the other hand, it does affect the visual appearance of the phase transfer curve in Fig. 2 and in similar plots in Figs. 3 and 4. In fact, subtraction of this term allows visual identification of a plateau in those curves, which is where amplitude fluctuations of the input signal affect the output phase the least (if at all).

The output phase of a given pulse has two contributions. One is due to XPM and is determined by the time-averaged power (i.e., in essence, by the average over powers of all pulses). The other contribution occurs due to SPM and is determined by the peak power of just that one pulse (see (5)). For an input with amplitude jitter, these contributions are *independent* since relation (6) does not hold in this case. We want to isolate the contribution due to SPM because it describes the *relative* phases of regenerated pulses whose input powers fluctuate about a given value. As noted in the previous paragraph, it is this relative phase that determines the eye opening of the regenerated signal. Therefore, in (11) we subtract the contribution due to the time-averaged power, which does not affect the relative phase between two pulses, and hence, the eye opening.

It remains to explain why one needs to use the coefficient "2" in front of the subtracted term. That is, why does one need to subtract the *sum* of the XPM contributions to the phases ϕ_3 and ϕ_4 and not, say, their mean value? We will present a calculation for the conventional coupler, whose output is given by (10). Calculations for a modified coupler with $\mu \neq 0$ and $\Delta \neq 0$ are more technical but lead to the same conclusion. We will use the following shorthand notations:

$$\alpha = \cos^2 \kappa z, \quad \beta = \sin^2 \kappa z, \quad |E_{3\text{in}}|^2 = \alpha|E|^2, \quad |E_{4\text{in}}|^2 = \beta|E|^2, \tag{A.1}$$

where the last two formulae follow from (3) when $\mu = \Delta = 0$. We will distinguish the peak power of the input pulse, $P = |E|^2$, from the time-averaged power, $\overline{P} = \overline{|E|^2}$. In addition, to emphasize the role of the coefficient "2" in (11), we will work not with that expression but with its generalization where the "2" is replaced by an arbitrary coefficient K:

$$\arg(E_{2\text{out}}) - K\gamma L \left(\overline{|E_{3\text{in}}|^2} + G\overline{|E_{4\text{in}}|^2} \right) \equiv \arg(E_{2\text{out}}) - K\gamma L(\alpha + G\beta)\overline{P}. \tag{A.2}$$

Thus, we will show why one should set $K = 2$ in the phase definition (A.2).

Recall that we want to isolate the contribution to the phase due to SPM from that due to XPM. A measure of whether the SPM contribution to the phase has a plateau with respect to the *peak power of an individual pulse* is the derivative of expression (A.2) with respect to the peak power P, which is to be computed while treating the time-averaged power $\overline{P}$ as a constant. The result, using (A.2), (10), (5), and (A.1), is:

$$\left.\frac{\partial\,(A.2)}{\partial P}\right|_{\overline{P}=\text{const}} = \gamma L \frac{\alpha^3 + G\beta^3 - \alpha\beta(\alpha + G\beta)\cos(\phi_3 - \phi_4)}{\alpha^2 + \beta^2 - 2\alpha\beta\cos(\phi_3 - \phi_4)}\,. \tag{A.3}$$

Next, at least ideally, one would like the plateau in the phase transfer curve defined by (A.2) — which *can be visualized* — to coincide with the plateau in the contribution to the phase due to SPM mentioned above, — which cannot be extracted from (A.2) and hence cannot be visualized. The plateau of the expression (A.2) with respect to the *pulse peak power plotted in the horizontal axis in Figs. 2, 3, and 5* is found where the slope of the corresponding curve vanishes. That slope is computed as the derivative of (A.2) with respect to the input peak power P, where now *the time-averaged power is related to the peak power by* (6): $\overline{P} = Pd$. Thus:

$$\left.\frac{d\,(A.2)}{d P}\right|_{\overline{P}=Pd} = \gamma L \frac{\alpha^2 c_1 + \beta^2 c_2 - \alpha\beta(\alpha + G\beta)c_3\cos(\phi_3 - \phi_4)}{\alpha^2 + \beta^2 - 2\alpha\beta\cos(\phi_3 - \phi_4)}\,, \tag{A.4a}$$

$$c_1 = \alpha(1-Kd)+G\beta d(2-K), \qquad c_2 = G\beta(1-Kd)+\alpha d(2-K), \quad c_3 = 1+2(1-K)d. \tag{A.4b}$$

Expressions (A.3) and (A.4) are proportional only when $K = 2$, in which case

$$\left.\frac{d\,(A.2)}{d P}\right|_{\overline{P}=Pd} = (1-2d)\,\left.\frac{\partial\,(A.2)}{\partial P}\right|_{\overline{P}=\text{const}}\,. \tag{A.5}$$

Thus, the plateau in the phase transfer curve coincides with the power range where the SPM contribution to the phase vanishes only when the phase is defined by (11).

References

[1] O. Leclerc, B. Lavigne, D. Chiaroni, E. Desurvire, "All-optical regeneration: Principles and WDM implementation," in I. Kaminow, T. Li (Eds.), Optical Fiber Telecommunications IVA: Components, San Diego, Academic Press, 2002, pp. 732–783.

[2] P.V. Mamyshev, "All-optical regeneration based on self-phase modulation effect," in Proceedings of the 24th European Conference on Optical Communications (ECOC), Madrid, Spain, 1998, vol. 1, pp. 475–476.

[3] J.T. Mok, J.L. Blows, B.J. Eggleton, "Investigation of group delay ripple distorted signals transmitted through all-optical 2R regenerators," Opt. Express 12 (2004) 4411–4422.

[4] V.G. Taèed, M. Shokooh-Saremi, L.B. Fu, I.C.M. Littler, D.J. Moss, M. Rochette, B.J. Eggleton, Y.L. Ruan, B. Luther-Davies, "Self-phase modulation-based integrated optical regeneration in chalcogenide waveguides," IEEE J. Sel. Top. Quantum Electron. 12 (2006) 360–370.

[5] N.J. Doran, D. Wood, "Nonlinear-optical loop mirror," Opt. Lett. 13 (1988) 56–58.

[6] S. Boscolo, S.K. Turitsyn, K.J. Blow, "Nonlinear loop mirror-based all-optical signal processing in fiber-optic communications," Opt. Fiber Technol. 14 (2008) 299–316.

[7] A.G. Striegler, M. Meissner, K. Cvecek, K. Sponsel, G. Leuchs, B. Schmauss, "NOLM-based RZ-DPSK signal regeneration," IEEE Photon. Technol. Lett. 17 (2005) 639–641.

[8] S. Boscolo, R. Bhamber, and S.K. Turitsyn, "Design of Raman-based nonlinear loop mirror for all-optical 2R regeneration of differential phase-shift-keying transmission," IEEE J. Quantum Electron. 42 (2006) 619–624.

[9] K. Cvecek, K. Sponsel, G. Onishchukov, B. Schmauss, G. Leuchs, "2R-regeneration of an RZ-DPSK signal using a nonlinear amplifying loop mirror," IEEE Photon. Technol. Lett. 19 (2007) 146–148.

[10] K. Cvecek, K. Sponsel, R. Ludwig, C. Schubert, C. Stephan, G. Onishchukov, B. Schmauss, G. Leuchs, "2R-regeneration of an 80-GB/s RZ-DQPSK signal by a nonlinear amplifying loop mirror," IEEE Photon. Technol. Lett. 19 (2007) 1475–1477.

[11] K. Sponsel, K. Cvecek, C. Stephan, G. Onishchukov, B. Schmauss, G. Leuchs, "Optimization of a nonlinear amplifying loop mirror for amplitude regeneration in phase-shift-keyed transmission," IEEE Photon. Technol. Lett. 19 (2007) 1858–1860.

[12] J.P. Gordon, L.F. Mollenauer, "Phase noise in photonic communications systems using linear amplifiers," Opt. Lett. 15 (1990) 1351-1353.

[13] C. Stephan, K. Sponsel, G. Onishchukov, B. Schmauss, G. Leuchs, "Phase preserving amplitude regeneration in DPSK transmission systems using a nonlinear amplifying loop mirror," IEEE J. Quantum Electron. 45 (2009) 1336–1343.

[14] O. Pottiez, E.A. Kuzin, B. Ibarra-Escamilla, J.T. Camas-Anzueto, F. Guttierez-Zainos, "Easily tunable nonlinear optical loop mirror based on polarization asymmetry," Opt. Express 12 (2004) 3878–3887.

[15] T. Sakamoto, K. Kikuchi, "Nonlinear optical loop mirror with an optical bias controller for achieving full-swing operation of gate switching," IEEE Photon. Technol. Lett. 16 (2004) 545–547.

[16] R.C. Youngquist, L.F. Stokes, H.J. Shaw, "Effects of normal mode loss in dielectric waveguide directional couplers and interferometers," IEEE J. Quantum Electron. 19 (1983) 1888–1896.

[17] A.W. Snyder, "Coupled-mode theory for optical fibers," J. Opt. Soc. Am. 62 (1972) 1267–1277.

[18] W.-P. Huang, "Coupled-mode theory for optical waveguides: an overview," J. Opt. Soc. Am. A 11 (1994) 963–983.

Captions to the Figures

1. Schematics of the NALM-based regenerator.

2. Power (a) and phase (b) transfer curves of the earlier studied model with a "conventional" coupler with no core mismatch and no dissipation ($\Delta = 0$, $\mu = 0$). The solid and dotted lines correspond to the dispersionless and dispersive cases considered in Secs. 2 and 3, respectively. Parameter κz equals 0.33 and 0.38 in the dispersionless and dispersive cases, respectively, and the other parameters are specified in the text.

3. Power (a), (c) and phase (b), (d) transfer curves of a dispersionless regenerator employing the modified coupler with: $\kappa z = 1.3$, $x = 1.0$ (a), (b); $\kappa z = 1.6$, $x = 0.85$ (c), (d). The solid and dashed curves correspond to $y = 0.2$ and $y = 0.3$, respectively. Note that the horizontal scale here is in milliwatts, while in Fig. 2 it is in watts.

4. Same as in Fig. 3, but for a NALM with fiber dispersion of -2 ps/nm/km.

5. Electrical eye diagrams of the input (a) and regenerated (b), (c) signals. For (b): $x = y = 0$ (the conventional coupler), $\kappa z = 0.38$, average (over all pulses) peak $|E|^2 = 220$ mW; for (c): $x = 1.0$, $y = 0.2$, $\kappa z = 1.3$, average peak $|E|^2 = 2.6$ mW.

6. (a) Minimum and maximum x-values of the modified coupler for which the regenerator produces eye opening of at least 1.0 dB; (b) the corresponding input powers. Solid, dashed, and dotted lines correspond to $y = 0.2$, 0.3, and 0.4, respectively.